THE JOURNAL OF PHYSICAL CHEMISTRY B

Article

pubs.acs.org/JPCB

Molecular Sinkers: X-ray Photoemission and Atomistic Simulations of Benzoic Acid and Benzoate at the Aqueous Solution/Vapor Interface

Niklas Ottosson,*[,†,∥] Anastasia O. Romanova,[‡,⊥] Johan Söderström,[†] Olle Björneholm,[†] Gunnar Öhrwall,[§] and Maxim V. Fedorov*[,‡,⊥]

[†]Department of Physics and Astronomy, Uppsala University, SE-751 20 Uppsala, Sweden

[‡]Max Planck Institute for Mathematics in the Sciences, Inselstrasse 22, D 04103, Leipzig, Germany

[§]MAX-lab, Lund University, Box 118, SE-221 00 Lund, Sweden

Supporting Information

ABSTRACT: In this work, we provide a detailed microscopic picture of the behavior of benzoic acid at the aqueous solution/vapor interface in its neutral as well as in its dissociated form (benzoate). This is achieved through a combination of highly surface-sensitive X-ray photoelectron spectroscopy experiments and fully atomistic molecular simulations. We show that significant changes occur in the interface behavior of the neutral acid upon release of the proton. The benzoic acid molecules are found to be strongly adsorbed at the interface layer with the planes of the aromatic rings oriented almost parallel to the water surface. In contrast, in the benzoate form, the carboxylate group shows a sinker-like behavior while the aromatic ring acts as a buoy, oriented nearly perpendicular to the surface. Furthermore, a significant fraction of the molecular ions move from the interface layer into the bulk of the solution. We rationalize these findings in terms of the very different hydration properties of the carboxylic group in the two charge states. The molecule has an amphiphilic nature, and the deprotonation thus changes the hydrophobic/hydrophilic balance between the nonpolar aromatic and the polar carboxylic parts of the molecule. That, consequently, leads to a pronounced reorientation and depletion of the molecules at the interface.

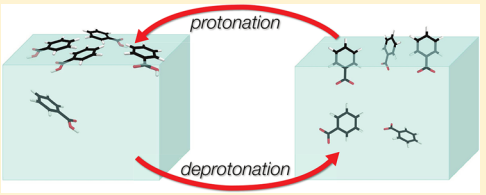

INTRODUCTION

Understanding the behavior of benzoic acid and other aromatic carboxylic acids (ACAs) at interfaces is important in many areas involving catalysis, environmental chemistry, and food and agricultural industries. Because benzoic acid is the most elementary representative of ACAs, its interface adsorption properties have been intensively studied by different experimental and modeling techniques for more than a century.[1−18] However, the molecular mechanisms of interface adsorption of benzoic acid and other ACAs still require a better understanding.

Here we present a combined experimental and theoretical study of the behavior of benzoic acid at the aqueous solution/vapor interface using X-ray photoelectron spectroscopy complemented by fully atomistic molecular simulations.

Benzoic acid has a pK_a of 4.21 in water, and at neutral pH, the carboxylic group of the molecule is thus primarily deprotonated, i.e., the molecule is in the form of the benzoate anion (when referring to a specific charge state of benzoic acid, we will in the following denote the neutral acid molecule as BAH and the benzoate anion as BA^-). Knowledge of the effects of protonation/deprotonation on the molecular structure of the benzoic acid aqueous solution/vapor interface is important for understanding the molecule's environmental effects, its transport and adsorption properties in technological processes, and its photo- and biodegradation in natural and industrial environments.[9,10,12,14,16,19−27] However, we are not yet aware of any molecular-scale study of the behavior of benzoic acid at the aqueous solution/vapor interface that makes a detailed comparison of the interface behavior of benzoic acid in different protonation states. This work fills parts of this gap and presents a molecular-scale picture of the behavior of both BAH and BA^- forms of benzoic acid at the aqueous solution/vapor interface.

Few spectroscopic techniques are available to study the orientation of molecules and molecular ions at the aqueous solution surface. X-ray photoelectron spectroscopy (XPS), especially in combination with tunable synchrotron radiation, is ideally suited to quantify the relative abundance of atoms in chemically inequivalent binding environments near a free surface. Therefore, XPS has become a standard tool in surface science for studies of the chemical state, coverage, and orientation of adsorbates on solid surfaces.[28,29] However, until recently, it was not possible to perform photoemission studies of aqueous solutions due to their high vapor pressures. This problem was overcome by the development of the liquid-jet technique,[30] which is utilized in the present study.

In 1s core-level photoemission, as performed here, the photoelectron spectrum can be considered as the sum of the individual emission contributions from the respective atomic sites, due to the high degree of localization of the 1s core-

Received: January 30, 2012
Revised: August 6, 2012
Published: August 30, 2012

   dx.doi.org/10.1021/jp300956j | J. Phys. Chem. B 2012, 116, 13017−13023

electrons on individual atoms. Further, the inelastic scattering of electrons in the condensed phase causes an exponential attenuation of the signal from an emitting site as a function of its distance from the solution surface. These factors taken together enable information about the spatial distribution of chemically inequivalent atomic sites near the water surface to be obtained through analysis of the intensities in the associated photoemission (PE) spectrum. This approach has been utilized in a number of recent photoemission studies. One line of investigation, followed by several research groups, has been to use XPS to probe spatially inhomogeneous distributions of simple inorganic ions near the water/vapor interface. In 2005, Ghosal et al. showed that iodide has a higher propensity for the surface layer than its potassium counterions in KI-crystals at humidities close to the deliquescence point.[31] Using a similar experimental approach, other studies of more complicated systems followed.[32,33] Important for the present study was also the demonstration of Nolting et al. in 2007 that organic conjugate acids and bases in solution can be well distinguished by XPS core-electron chemical shifts.[34] Recent works have drawn use of these possibilities to determine the degree of protonation of weak acids and bases at the water/vapor interface.[35,36] These results also suggest that it should be possible to extract information about the orientation of organic acids and bases at the aqueous interface from their XPS spectra.[32,37,38]

Combining results from photoelectron spectroscopy with fully atomistic molecular dynamics simulations has great potential, as photoelectron intensity distributions can be calculated from simulated density profiles, employing simple attenuation models. Hence, the validity of the simulations can be evaluated and the comparison with the photoemission experiments can yield substantial information about the orientation and distribution of different solutes at the aqueous solution/vapor interface.

METHODS

Liquid-Jet X-ray Photoelectron Spectroscopy. The liquid-jet photoelectron experiments were performed at the Swedish national synchrotron facility MAX-lab, Lund, at the soft X-ray undulator beamline I411.[39] The experimental setup has previously been described in detail.[40] Briefly, the liquid samples are injected into an evacuated experimental chamber as a 20 μm jet, traveling at a velocity of approximately 25 m/s. The ionization occurs within a few millimeters after injection, whereafter the liquid jet is frozen out in a liquid nitrogen cold trap. The expelled electrons enter the analyzer through a circular opening with a diameter of ~0.5 mm, situated approximately 2 mm from the liquid surface. This allows for good differential pumping of the spectrometer, while a sufficiently small fraction of the photoelectrons is lost in the short passage through the vapor. The electron analyzer is mounted perpendicular to the flow of the jet and at an angle of 54.7° (the so-called magic angle) to the linearly polarized synchrotron radiation, in order to minimize the influence of anisotropic angular distribution effects.[28]

The total experimental resolution was better than 250 meV at 360 eV photon energy, determined from the width of the gas phase water $1b_1$ state, i.e., significantly smaller than the inherent widths of the investigated photoelectron lines. Their substantial line width is dominated by inhomogeneous broadening contributions, arising from the range of inequivalent hydration configurations in the solution. Samples were prepared fresh before each experiment to 10 mM concentration from highly demineralized water (18.2 MΩ, Millipore Direct-Q) and commercially obtained benzoic acid (Puriss P.A., Fluka, >99.5%). Sodium benzoate was prepared by adding concentrated NaOH to a solution of benzoic acid until a pH of 10.2 was reached; the pH was monitored using a calibrated pH-meter (Hanna pH 212) equipped with a Mettler Toledo Inlab Routine electrode. The binding energy (BE) scale has been calibrated against the $(1b_1)^{-1}$ state of liquid water,[41] which was monitored in parallel with the presented C1s photoelectron spectra.

Molecular Modeling. We have performed fully atomistic molecular dynamics (MD) simulations of separate water solutions of molecular benzoic acid and sodium benzoate using the Gromacs 4.5 package.[42−46] We used a similar methodology as in the previous studies of solvation effects on benzoic acid and an anionic polypeptide with carboxylic groups.[47] Benzoates were neutralized by sodium cations. We used the TIP4P model for water[48] and the OPLSAA-2005 force field[49−56] for organic compounds. Na^+ ions were described with parameters developed in ref 57. We simulated 20 BAH molecules in a box of 5437 H_2O molecules. For BA^- simulations, we used 87 BA^-−Na^+ pairs in a box of 4868 water molecules (sodium benzoate is more soluble than the molecular form). No restraints were applied on the systems. We used larger concentrations of BAH and BA^- in our simulations than in the experiments because the experimental concentrations are too small (10 mM) for molecular simulations to collect reasonable statistics of molecular distributions at the surface.

Simulations were carried out in two steps for all systems. During the first step, we equilibrated the systems in the NPT ensemble for 1 ns. Before the equilibration runs, the potential energy of every system was minimized using the energy minimization procedure to avoid sterical clashes between the atoms. Then, we performed productive runs in the NVT ensemble at constant T = 300 K in a slab geometry with PME electrostatics using the Yeh and Berkowitz correction[58,59] for slab geometry. To collect sufficient statistics of benzoic acid adsorption, we simulated all systems for 55 ns and considered the last 45 ns for analysis.

More details about the simulation setup and verification of the simulation protocol can be found in the Supporting Information to this paper.

RESULTS AND DISCUSSION

Figure 1a and b shows the C1s photoelectron spectra of 10 mM aqueous benzoic acid and 10 mM sodium benzoate, respectively. Both spectra were recorded at 360 eV excitation energy. The resulting photoelectron kinetic energies of 65−70 eV lie near the minimum of the photoelectron inelastic mean free path function (on the order of 1 nm), making these measurements highly surface sensitive.[28,60] Each spectrum was fitted with an appropriate number of Voigt functions using a least-squares approach. The Lorentzian lifetime widths were fixed for all lines with values obtained from the literature,[61] while the respective Gaussian widths were free to vary. The resulting fits are shown in each panel as a solid line, superimposed on the experimental data, while the individual components are given as thinner lines, rising from the residue (blue dashed line). In order to improve visual clarity, a linear background has been subtracted from each spectrum.

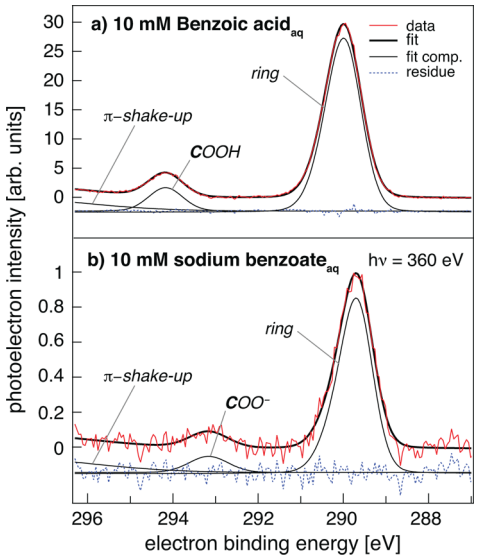

Figure 1. C1s photoelectron spectra of (a) 10 mM benzoic acid and (b) 10 mM sodium benzoate in aqueous solution taken at 360 eV photon energy. Each spectrum clearly separates contributions from the carboxylic/carboxylate carbons and aromatic ring carbons. Since the spectra are highly surface sensitive, deviations from the stoichiometric signal intensity proportions are indicative or preferential surface orientations.

The C1s spectra of both benzoic acid (Figure 1a) and benzoate (Figure 1b) can be decomposed into two main regions: that of the carboxylic/carboxylate carbons at higher BE, and a more intense feature at lower BE, arising from core-emission of the aromatic ring. At the high-energy tail, the onset of an additional broad feature is observed: we attribute this to shake-up processes of the aromatic π-system, which have been thoroughly studied in the gas phase.[62,63] The shift of the carboxylic line of about 4 eV relative to the ring carbons enables a reliable quantification of the respective peak intensities from BAH and BA^-, which is crucial in the current experiment, as we are interested in the molecular orientation as a function of protonation state.

The carboxylic C1s line of BAH, shown in Figure 1a, is found at 294.2 eV BE, while photoemission from the carboxylate carbons of BA^- is shifted to lower BEs by ~1.1 eV relative to the acid form. This shift is similar to what has been found from photoemission of the carboxylate group of simple carboxylic acids in aqueous solution,[35] as well as the hydrated amino acids.[34,64] While the aromatic ring of BAH and BA^- contains four types of chemically inequivalent carbons (first, *ortho-*, *meta-*, and *para-*), the binding energy shifts between these spectral features are obviously too small to allow a reliable separation. The whole ring feature of BAH can indeed be well fitted with a single Voigt function, centered at ~290.0 eV, while the fit improves slightly if an additional weak feature is added on the high-BE side (at 290.4 eV). For BA^-, the ring carbon BEs are less affected by the deprotonation than the BE of the carboxylic group, as can be expected given that they are farther away from the deprotonated site; the peak is centered around 289.7 eV. Since we are not going to attribute the present decomposition of the ring features any definite physical significance, and given that we are primarily interested in the intensity ratio between the ring and carboxylic/carboxylate PE features, we show the resulting fit of the ring structure as one single component in Figure 1a and b.

As can be seen in Figure 1, the ring carbon C1s signal from the BAH solution is approximately a factor of 30 stronger than that from the equimolar solution of sodium benzoate; note that the arbitrary units of the photoelectron intensity are the same in Figure 1a and b. On the basis of this observation alone, we conclude that undissociated BAH is significantly surface enriched relative to its conjugate base form BA^-. We also note that this is the reason behind the marked difference in signal-to-noise ratios in the spectra of BAH and BA^-.

We will now focus on the C1s spectral intensity distributions obtained from the respective charge state. For benzoic acid, the ring/carboxylic PE ratio is found to be 7.86 ± 0.01, from the fits shown in the figure, i.e., ~30% higher than the stoichiometric ratio of 6:1. This value increases for sodium benzoate; the ring/carboxylate PE ratio is now instead 10.1 ± 0.7, i.e., as much as 70% higher than what would have been expected from simple stoichiometric considerations. What do these photoelectron spectra tell us about the orientation of BAH and BA^- at the water/vapor interface? If we were to assume that the photoionization cross section is the same for the two types of carbons, we would expect to retrieve the stoichiometric proportions if the molecules were totally randomly oriented, or lying totally flat on the surface. By the same token, deviations from a ratio of 6 (as is the case for both BAH and BA^-) would then signify surface orientation of the molecules. However, we cannot exclude that the significantly higher values of the PE ratios than expected from stoichiometry, at least partly, originates from cross section differences between the two types of carbon. While the C1s cross sections of inequivalent carbons far above the ionization threshold to a good approximation are identical, this is not necessarily the case at low excess energies. Recently, it has been demonstrated that photoemission intensity from carbon atoms close to heavy halide atoms in substituted hydrocarbons can be severely modulated and shows a marked photon energy dependence up to several hundred electronvolts of kinetic energy.[65] This "EXAFS-like" effect can be understood as arising from scattering of the outgoing photoelectron on the neighboring halide atoms. Such dramatic effects are however not expected for BAH and BA, given that none of the carbons are binding to any heavier element, and only a weak modulation is potentially expected. Most importantly, when comparing ring/carboxylic PE ratios from the two forms, the only difference is that of a single proton, which is a very weak photoelectron scatterer. Hence, we conclude that the significant *increase* of the experimentally observed ring/carboxylic PE ratio upon deprotonation only can signify that interfacial benzoate anions are more strongly oriented with the aromatic rings pointing out toward the gas phase while the carboxylate groups are sticking into the aqueous solvent, compared to the neutral form of benzoic acid.

In order to better understand the origins of the PE intensity distributions, and to investigate the molecular-level details of the surface orientation of BAH and BA^-, we have performed fully atomistic MD simulations of BAH and BA^- in a slab of water. Figure 2 shows converged density profiles of the aromatic ring/carboxylic carbons and the water solvent in the water/vapor interface layer, obtained from simulations of benzoic acid (panel a) and sodium benzoate (panel b) in the slab geometry. The respective water, ring carbon, and carboxylic/carboxylate carbon density profiles have been normalized so that unity designates the nominal concentration of the species under ideal mixing.

dx.doi.org/10.1021/jp300956j | J. Phys. Chem. B 2012, 116, 13017−13023

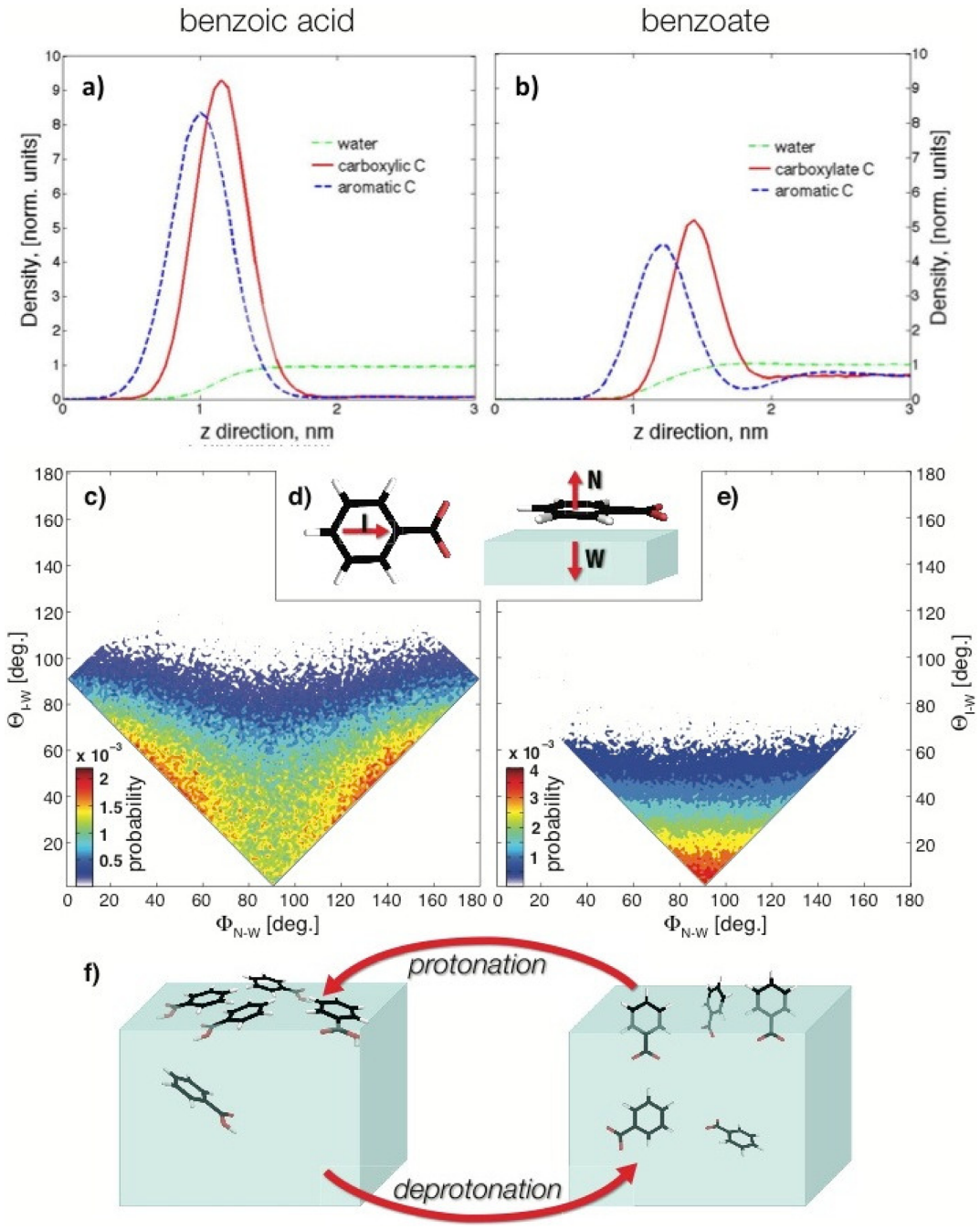

Figure 2. Molecular orientations in the surface layer of aqueous BAH/BA$^-$ solutions from MD simulations. (a, b) Normalized density profiles of the aromatic ring/carboxylic carbons and the water solvent, respectively, in the direction perpendicular to the water surface. (c, e) Angle distributions of BAH/BA$^-$, respectively, in the surface layer, normalized with Jacobian determinant of the angular transformation. Insertion (d) shows definitions of the molecular orientation vectors **I** and **N**, where **W** is the vector perpendicular to the water surface. (f) Pictorial representation of the BAH/BA$^-$ behavior in the surface layer upon protonation/deprotonation.

Consistent with the photoemission data, the neutral acid (panel a) is found to be strongly surface segregated in the simulations; the surface concentration of BAH is much higher than in the bulk. We also note that the carboxylic and ring carbon densities to a large extent overlap in the *z*-direction, with a slight shift of the ring carbon profile toward the surface, showing that the molecules have a close to flat surface orientation with a weak preference of pointing the carboxylic groups into the aqueous phase (see Figure 2c and f); see also the Supporting Information to the paper). While the BA$^-$ (panel b) is also surface enriched, but less so than BAH, a considerable amount of the molecular anions are found in the interior of the slab. This result is consistent with the drop of the C1s PE signal upon dissociation of BAH (compare Figure 1a and b). In line with the experimental results, the density profiles from MD simulations presented in Figure 2b show a pronounced spatial separation between the aromatic and the carboxylate carbons in the *z*-direction; the latter site (COO^-) is pointing into the water bulk.

While it is clear from the discussions above that the MD simulations are in good qualitative agreement with the photoemission experiments, the connection can be made

dx.doi.org/10.1021/jp300956j | *J. Phys. Chem. B* 2012, 116, 13017−13023

more explicit in various ways. We have here chosen to employ a simple attenuation model, as described in ref 60, to simulate the expected PE intensity ratios from the simulated density profiles, as a function of the electron inelastic mean free path in the aqueous phase. The details of the procedure and results are given in the Supporting Information. The agreement, while not fully quantitative, is fair. Most importantly, the relative change in the PE ratio upon going from BAH to BA^- is well captured in the simulations.

Assured that the MD simulations are consistent with the photoemission experiment, we move on to a more detailed analysis of the range of surface conformations present in the respective simulated trajectories. To describe the orientation of BAH/BA^- relative to the water surface, we have defined two molecular vectors: The first, **I**, lies in-plane in the direction from the center of the *para*-C atom to the center of the $COOH/COO^-$ group carbon atom, while the other, **N**, is normal to the molecular plane. Both vectors are shown graphically in Figure 2d together with the normal vector **W** to the water surface. The orientation of an individual molecule can thus be conveniently described in terms of a pair of angles, Θ_{I-W}, which denotes the angle formed between **I** and **W**, and Φ_{N-W}, which is the angle between **N** and **W**. In other words, the angle Θ_{I-W} describes $COOH/COO^-$ molecular site orientation and Φ_{N-W} describes the orientation of the molecular plane with respect to the water surface plane. In terms of these geometrical parameters, parts c and e of Figure 2 show angular distribution maps for benzoic acid and benzoate, respectively, near the aqueous solution/vapor interface. Note that, due to the orthogonality of the vectors **I** and **N**, only geometries within a 45° tilted quadratic area are allowed. The corners of the square are situated at the center on the Φ_{N-W} and Θ_{I-W} axes. To overcome the problem with non-uniform probability distribution of the conformations, the distributions in Figure 2c and e have been normalized with the Jacobian determinant of the angular transformation (see the Supporting Information for details).

The pronounced differences in surface orientation between BAH and BA^- are revealed in great detail in Figure 2c and e. As already deduced from the density profiles in Figure 2a and b, a considerable amount of the neutral acid molecules are lying nearly flat on the surface with a tendency for the carboxylic group to point into the solution, resulting in considerable intensity peak around $\Theta_{I-W} \approx 50°$. Furthermore, most of these configurations have an angle Φ_{N-W} near the bottom-right/bottom-left edges of the surfaces in Figure 2c, which corresponds to a simple tilt of the COOH-terminal into the solution, without rotation of the molecule. Configurations around $\Phi_{N-W} = 90°$, which correspond to the molecular orientation such that the aromatic ring has been rotated perpendicular to the water surface, are much less present.

A rather detailed picture of the surface orientation of benzoic acid is emerging: The pronounced surface segregation of BAH is driven by hydrophobic interactions. In the surface layer, BAH however preferentially aligns the hydrophobic aromatic ring so that its electronic π-system can interact with the polar solvent at one side. This makes parallel configurations favorable compared to perpendicular ones. The carboxylic group, on the other hand, can form somewhat stronger hydrogen donor bonds with the solvent, which is hard to satisfy in a fully parallel geometry with the surface. This represents a driving force for the molecule to tilt into the aqueous phase with the carboxylic group pointing downward. The angular distribution shown in Figure 2c is thus the result of balancing these counteracting tendencies in the surface hydration of benzoic acid; see the pictorial representation of the surface layer, given in Figure 2f, left part.

Benzoate on the other hand shows a maximum of the probability density centered near $\Theta_{I-W} = 0°$, $\Phi_{N-W} = 90°$, i.e., when the COO^- groups point directly down into the solution; see pictorial representation in the right part of Figure 2f. Furthermore, as was shown in Figure 2b, the deprotonation also results in a decrease of the overall surface excess. We conclude that the carboxylate group of BA^- shows a sinker-like behavior, due to the efficient hydration of the ionic group, while the hydrophobic aromatic ring acts as a buoy, keeping a significant part of the molecular ions close to the interface.

In support of our findings, we note that in several studies it has been shown that the pH level of aqueous benzoic acid solutions (and, hence, the degree of dissociation of the acid) strongly influences the adsorption properties of the molecule at interfaces. For example, Ishikawa et al. investigated the adsorption of aromatic carboxylic acids into low-density polyethylene films as a function of pH.[19] They showed that the adsorption level of benzoic acid to the film increased with decreasing pH. There are also studies of orientation properties of ACAs at interfaces. As an example, the electrochemical studies of benzoic acid behavior on platinum and gold electrodes by Montilla et al. suggest that the aromatic ring of the benzoate anion is preferentially oriented perpendicular to the water−electrode interface.[20]

Benzoic acid is an amphiphilic compound with a hydrophobic aromatic ring and a hydrophilic carboxylic group. BAH and BA^- differ by the charge state of the carboxylic functional group, which causes their different behavior at the aqueous solution/vapor interface. It is known that nonsubstituted aromatic systems tend to lie flat on the water surface.[66−69] Substitution of one aromatic proton by a weakly hydrated COOH group apparently does not significantly affect the flat orientation, which is driven by the interaction of the aromatic ring's electronic π-system with the water solvent (the BAH surface orientation is only slightly tilted, see Figure 2). However, deprotonation of the carboxylic group drastically changes the balance of hydration energies for the hydrophobic and hydrophilic parts of the molecule. The strongly hydrophilic carboxylate part of BA^- tends to be fully immersed in water because of the high energetic gain upon full hydration of this anionic group. The drastic change of the hydrophobic/hydrophilic balance also leads to a reduced benzoate concentration at the surface compared to that of the strongly surface segregated molecular BAH form.

CONCLUSIONS

Our strategy of combining X-ray photoelectron spectroscopy with fully atomistic MD simulations has allowed us to investigate the molecular mechanisms of the adsorption at the water−air interface of benzoic acid in detail. We have shown that drastic changes in the interface behavior take place when the acid dissociates into the benzoate anion. Comparative analysis of experimental C1s PE intensities for protonated/deprotonated forms of benzoic acid and the results of direct atomistic simulations of the BAH/BA^- molecules at the water−air interface suggests that

(i) the BAH molecules are mainly adsorbed in the interface layer rather than in the bulk with the aromatic rings oriented parallel to the water surface

dx.doi.org/10.1021/jp300956j | J. Phys. Chem. B 2012, 116, 13017−13023

(ii) converting the molecule to BA^- results in a sinker-like behavior of the carboxylate group, with the aromatic ring becoming perpendicular to the surface and acting as a buoy, still keeping a large fraction of the molecules in the interface region; moreover, a significant fraction of the molecules moves from the interface layer into the bulk.

We attribute the observed differences in interface behavior of the neutral and dissociated forms of benzoic acid to the changes in the hydration properties of the carboxylic group upon deprotonation. This changes the balance between the hydrophobic and hydrophilic structural motifs of the amphiphilic molecule, resulting in the flip of its interface orientation.

While the present study only concerned benzoic acid, the most elementary representative of the aromatic carboxylic acids, we believe that the mechanism revealed here is rather general, at least as a trend, for other molecules in this class. Recent surface specific measurements have clearly showed how the behavior of titratable molecules can be very different at the aqueous surface compared to in the bulk, and that this molecular surface structure can be of significant importance for other processes. For example, simple carboxylic acids were found to be considerably less dissociated at the interface than would be expected from their pK_a values alone,[35] which affects the surface tension of organic acid containing atmospheric aqueous aerosols as a function of pH in a nontrivial way. Similar observations were made for the weak base monoethanolamine, which was found to be more surface active than its cationic conjugate base form, a finding of significance for understanding the mechanistic details of CO_2 capture by amine-based aqueous solutions.[36]

Given the importance of the molecular surface structure for surface specific chemical reactions, the results presented here should thus have implications for many areas where surface/interfacial chemistry of aromatic carboxylic acids is involved. These include surface catalysis, atmospheric and environmental chemistry, pharmacology, and food chemistry.

■ ASSOCIATED CONTENT

Ⓢ Supporting Information

Further simulation details; the Jacobian determinant for the angular transformation of Figure 2; the structure preparation used in the MD simulations; estimates of ring/carboxylic C 1s PE ratio; calculations of the potential of mean force for the BAH molecule traveling along the *z*-direction. This material is available free of charge via the Internet at http://pubs.acs.org.

■ AUTHOR INFORMATION

Corresponding Author

*E-mail: n.ottosson@amolf.nl (N.O.); maxim.fedorov@strath.ac.uk (M.V.F.).

Present Addresses

[‖]FOM Institute AMOLF, Science Park 104, 1098 XG Amsterdam, The Netherlands.

[⊥]Department of Physics, Strathclyde University, John Anderson Building, 107 Rottenrow East, Glasgow, U.K. G4 0NG.

Notes

The authors declare no competing financial interest.

■ ACKNOWLEDGMENTS

We acknowledge the supercomputing support from Juelich Supercomputing Centre (JSC), Forschungszentrum Juelich GmbH, Germany. Project ID: ESMI11. A.O.R. was supported by Deutsche Forschungsgemeinschaft within the Graduate School BuildMoNa. A.O.R. and M.V.F. acknowledge support of Scottish Universities Physics Alliance (SUPA). J.S. acknowledges financial support from Knut and Alice Wallenberg's foundation.

■ REFERENCES

(1) Lehman, K. B. *Science* **1912**, *35*, 577−585.
(2) Long, J. H. *Science* **1913**, *37*, 395−404.
(3) Brul, S.; Coote, P. *Int. J. Food Microbiol.* **1999**, *50*, 1−17.
(4) Andersen, F. *Int. J. Toxicol.* **2001**, *20*, 23−50.
(5) Izumi, I.; Fan, F. R. F.; Bard, A. J. *J. Phys. Chem.* **1981**, *85*, 218−223.
(6) Tokunaga, M.; Larrow, J. F.; Kakiuchi, F.; Jacobsen, E. N. *Science* **1997**, *277*, 936−938.
(7) Chiong, H. A.; Pham, Q. N.; Daugulis, O. *J. Am. Chem. Soc.* **2007**, *129*, 9879−9884.
(8) Corrigan, D. S.; Weaver, M. J. *Langmuir* **1988**, *4*, 599−606.
(9) Mendez-Roman, R.; Cardona-Martinez, N. *Catal. Today* **1998**, *40*, 353−365.
(10) Augugliaro, V.; Coluccia, S.; Loddo, V.; Marchese, L.; Martra, G.; Palmisano, L.; Schiavello, M. *Appl. Catal., B* **1999**, *20*, 15−27.
(11) McCollom, T. M.; Seewald, J. S.; Simoneit, B. R. T. *Geochim. Cosmochim. Acta* **2001**, *65*, 455−468.
(12) He, J.; Ma, W.; Song, W.; Zhao, J.; Qian, X.; Zhang, S.; Yu, J. *Water Res.* **2005**, *39*, 119−128.
(13) Verduyn, C.; Postma, E.; Scheffers, W. A.; Vandijken, J. P. *Yeast* **1992**, *8*, 501−517.
(14) Natella, F.; Nardini, M.; Felice, M. D.; Scaccini, C. *J. Agric. Food Chem.* **1999**, *47*, 1453−1459.
(15) Chen, Q.; Richardson, N. V. *Prog. Surf. Sci.* **2003**, *73*, 59−77.
(16) de Jesus, M. A.; Giesfeldt, K. S.; Sepaniak, M. J. *Appl. Spectrosc.* **2004**, *58*, 1157−1164.
(17) Han, B.; Li, Z. H.; Wandlowski, T. *Anal. Bioanal. Chem.* **2007**, *388*, 121−129.
(18) Minofar, B.; Jungwirth, P.; Das, M. R.; Kunz, W.; Mahiuddin, S. *J. Phys. Chem. C* **2007**, *111*, 8242−8247.
(19) Ishikawa, H.; orthers. *J. Agric. Food Chem.* **2005**, *53*, 3488−3492.
(20) Montilla, F.; Morallon, E.; Vazquez, J. L. *Langmuir* **2003**, *19*, 10241−10246.
(21) Oda, H.; Kishida, M.; Yokokawa, C. *Carbon* **1981**, *19*, 243−248.
(22) Nicholson, J. K.; Wilson, I. D. *Nat. Rev. Drug Discovery* **2003**, *2*, 668−676.
(23) Franz, M.; Arafat, H. A.; Pinto, N. G. *Carbon* **2000**, *38*, 1807−1819.
(24) Kuzmenko, I.; Kindermann, M.; Kjaer, K.; Howes, P. B.; Als-Nielsen, J.; Granek, R.; von Kiedrowski, G.; Leiserowitz, L.; Lahav, M. *J. Am. Chem. Soc.* **2001**, *123*, 3771−3783.
(25) Natan, A.; Kronik, L.; Haick, H.; Tung, R. T. *Adv. Mater.* **2007**, *19*, 4103−4117.
(26) Perlovich, G. L.; Volkova, T. V.; Manin, A. N.; Bauer-Brandl, A. *J. Pharm. Sci.* **2008**, *97*, 3883−3896.
(27) Qin, W. C.; Sua, L. M.; Zhanga, X. J.; Qina, H. W.; Wena, Y.; Guoa, Z.; Suna, F. T.; Shenga, L. X.; Zhaoa, Y. H.; Abraham, M. H. *SAR QSAR Environ. Res.* **2010**, *21*, 389−401.
(28) Hüfner, S. *Photoelectron Spectroscopy*; Springer-Verlag: Berlin, Heidelberg, 1995.
(29) Nilsson, A. *J. Electron Spectrosc. Relat. Phenom.* **2002**, *126*, 3−42.
(30) Faubel, M.; Steiner, B.; Toennies, J. P. *J. Chem. Phys.* **1997**, *106*, 9013−9031.
(31) Ghosal, S.; Hemminger, J. C.; Bluhm, H.; Mun, B. S.; Hebenstreit, E. L. D.; Ketteler, G.; Ogletree, D. F.; Requejo, F. G.; Salmeron, M. *Science* **2005**, *307*, 563−566.
(32) Ghosal, S.; Brown, M. A.; Bluhm, H.; Krisch, M. J.; Salmeron, M.; Jungwirth, P.; Hemminger, J. C. *J. Phys. Chem. A* **2008**, *112*, 12378−12384.

(33) Ottosson, N.; Heyda, J.; Wernersson, E.; Pokapanich, W.; Svensson, S.; Winter, B.; Öhrwall, G.; Jungwirth, P.; Björneholm, O. *Phys. Chem. Chem. Phys.* **2010**, *12*, 10693−10700.
(34) Nolting, D.; Aziz, E.; Ottosson, N.; Faubel, M.; Hertel, I. V.; Winter, B. *J. Am. Chem. Soc.* **2007**, *129*, 14068−14073.
(35) Ottosson, N.; Wernersson, E.; Söderstrom, J.; Pokapanich, W.; Kaufmann, S.; Svensson, S.; Persson, I.; Öhrwall, G.; Björneholm, O. *Phys. Chem. Chem. Phys.* **2011**, *13*, 12261−12267.
(36) Lewis, T.; Faubel, M.; Winter, B.; Hemminger, J. C. *Angew. Chem., Int. Ed.* **2011**, *50*, 10178−10181.
(37) Weber, R.; Winter, B.; Schmidt, P. M.; Widdra, W.; Hertel, I. V. *J. Phys. Chem. B* **2004**, *108*, 4729−4736.
(38) Ottosson, N.; Vacha, R.; Aziz, E. F.; Pokapanich, W.; Eberhardt, W.; Svensson, S.; Öhrwall, G.; Jungwirth, P.; Björneholm, O.; Winter, B. *J. Chem. Phys.* **2009**, *131*, 124706.
(39) Bässler, M.; Forsell, J.-O.; Björneholm, O.; Feifel, R.; Jurvansuu, M.; Aksela, S.; Sundin, S.; Sorensen, S.; Nyholm, R.; Ausmees, A.; Svensson, S. *J. Electron Spectrosc. Relat. Phenom.* **1999**, *101−103*, 953−957.
(40) Bergersen, H.; Marinho, R. R. T.; Pokapanich, W.; Lindblad, A.; Björneholm, O.; Saethre, L. J.; Öhrwall1, G. *J. Phys.: Condens. Matter* **2007**, *19*, 326101.
(41) Winter, B.; Weber, R.; Widdra, W.; Dittmar, M.; Faubel, M.; Herte, I. V. *J. Phys. Chem. A* **2004**, *184*, 2625−2632.
(42) *GROMACS*; Biophysical Chemistry of Groningen University: Groningen, The Netherlands; www.gromacs.org.
(43) Berendsen, H. J. C.; van der Spoel, D.; van Drunen, R. *Comput. Phys. Commun.* **1995**, *91*, 43−56.
(44) Lindahl, E.; Hess, B.; B.; van der Spoel, D. *J. Mol. Model.* **2001**, *7*, 306−317.
(45) van der Spoel, D.; Lindahl, E.; Hess, B.; Groenhof, G.; Mark, A. E.; Berendsen, H. *J. Comput. Chem.* **2005**, *26*, 1701−1718.
(46) Hess, B.; Kutzner, C.; van der Spoel, D.; Lindahl, E. *J. Chem. Theory Comput.* **2008**, *435*, 435−447.
(47) M. V. Fedorov, J. M. G.; Schumm, S. *J. Am. Chem. Soc.* **2009**, *131*, 10854−10856.
(48) Jorgensen, W. L.; Chandrasekhar, J.; Madura, J. D.; Impey, R. W.; Klein, M. L. *J. Chem. Phys.* **1983**, *79*, 926−935.
(49) Jorgensen, W. L.; Maxwell, D. S.; Tirado-Rives, J. *J. Am. Chem. Soc.* **1996**, *118*, 11225−11236.
(50) Damm, W.; Frontera, A.; Tirado-Rives, J.; Jorgensen, W. L. *J. Comput. Chem.* **1997**, *18*, 1955−1970.
(51) Jorgensen, W. L.; McDonald, N. A. *J. Mol. Struct.* **1998**, *424*, 145−155.
(52) McDonald, N. A.; Jorgensen, W. L. *J. Phys. Chem. B* **1998**, *102*, 8049−8059.
(53) Rizzo, R. C.; Jorgensen, W. L. *J. Am. Chem. Soc.* **1999**, *121*, 4827−4836.
(54) Watkins, E. K.; Jorgensen, W. L. *J. Phys. Chem. A* **2001**, *105*, 4118−4125.
(55) Kaminski, G. A.; Friesner, R. A.; Tirado-Rives, J.; Jorgensen, W. L. *J. Phys. Chem. B* **2001**, *105*, 6474−6487.
(56) Jacobson, M. P.; Kaminski, G. A.; Friesner, R. A.; Rapp, C. S. *J. Phys. Chem. B* **2002**, *106*, 11673−11680.
(57) Jensen, K. P.; Jorgensen, W. *J. Chem. Theory Comput.* **2006**, *2*, 1499−1509.
(58) Yeh, Y.-C.; Berkowitz, M. L. *J. Chem. Phys.* **1999**, *111*, 3155−3162.
(59) Yeh, Y.-C.; Berkowitz, M. L. *J. Chem. Phys.* **2000**, *112*, 10491−10495.
(60) Ottosson, N.; Faubel, M.; Bradforth, S. E.; Jungwirth, P.; Winter, B. *J. Electron Spectrosc. Relat. Phenom.* **2010**, *177*, 60−70.
(61) Coville, M.; Thomas, T. D. *Phys. Rev. A* **1991**, *43*, 6053−6056.
(62) Lunell, S.; Svensson, S.; Malmqvist, P.-A.; Gelius, U.; Basilier, E.; Siegbahn, K. *Chem. Phys. Lett.* **1978**, *54*, 420−424.
(63) Keane, M. P.; de Brito, A. N.; Correia, N.; Svensson, S.; Lunell, S. *Chem. Phys.* **1991**, *155*, 379.
(64) Ottosson, N.; Børve, K. J.; Spångberg, D.; Bergersen, H.; Sæthre, L. J.; Faubel, M.; Pokapanich, W.; Öhrwall, G.; Björneholm, O.; Winter, B. *J. Am. Chem. Soc.* **2011**, *133*, 3120−3130.
(65) Söderström, J.; Mårtensson, N.; Travnikova, O.; Patanen, M.; Miron, C.; Sæthre, L. J.; Børve, K. J.; Rehr, J. J.; Kas, J. J.; Vila, F. D.; Thomas, T. D.; Svensson, S. *Phys. Rev. Lett.* **2012**, *108*, 193005.
(66) Pohorille, A.; Benjamin, I. *J. Chem. Phys.* **1991**, *94*, 5599−5605.
(67) Pohorille, A.; Benjamin, I. *J. Phys. Chem.* **1993**, *97*, 2664−2670.
(68) Benjamin, I. *Chem. Rev.* **1996**, *96*, 1449−1475.
(69) Vacha, R.; Cwiklik, L.; Rezac, J.; Hobza, P.; Jungwirth, P.; Valsaraj, K.; Bahr, S.; Kempter, V. *J. Phys. Chem. A* **2008**, *112*, 4942−4950.